AWARD NUMBER: W81XWH-20-1-0667

TITLE: Determinants of Basal Forebrain Cholinergic Neuron Vulnerability in Parkinson's Disease and Lewy Body Dementia

PRINCIPAL INVESTIGATOR: Dalton James Surmeier

CONTRACTING ORGANIZATION: Northwestern University, Evanston, IL

REPORT DATE: August 2023

TYPE OF REPORT: Annual

PREPARED FOR: U.S. Army Medical Research and Development Command
Fort Detrick, Maryland 21702-5012

REPORT DOCUMENTATION PAGE

Form Approved
OMB No. 0704-0188

1. REPORT DATE	2. REPORT TYPE	3. DATES COVERED
August 2023	Annual	01Aug2022-31Jul23

4. TITLE AND SUBTITLE

Determinants of Basal Forebrain Cholinergic Neuron Vulnerability in Parkinson's Disease and Lewy Body Dementia

5a. CONTRACT NUMBER
W81XWH-20-1-0667

5b. GRANT NUMBER
PD190086

5c. PROGRAM ELEMENT NUMBER

6. AUTHOR(S)

Dalton James Surmeier

E-Mail: j-surmeier@northwestern.edu

5d. PROJECT NUMBER
0011470539-0001

5e. TASK NUMBER

5f. WORK UNIT NUMBER

7. PERFORMING ORGANIZATION NAME(S) AND ADDRESS(ES)

NORTHWESTERN UNIVERSITY
633 CLARK ST
EVANSTON IL 60208-0001

8. PERFORMING ORGANIZATION REPORT NUMBER

9. SPONSORING / MONITORING AGENCY NAME(S) AND ADDRESS(ES)

U.S. Army Medical Research and Development Command
Fort Detrick, Maryland 21702-5012

10. SPONSOR/MONITOR'S ACRONYM(S)

11. SPONSOR/MONITOR'S REPORT NUMBER(S)

12. DISTRIBUTION / AVAILABILITY STATEMENT

Approved for Public Release; Distribution Unlimited

13. SUPPLEMENTARY NOTES

14. ABSTRACT

Parkinson's disease (PD) poses one of the greatest healthcare challenges of our time. With the aging of the general population, the incidence of PD is expected to rise in coming decades. This wave will create not only a humanitarian crisis, but an unsustainable tax on societal resources. Although there are effective symptomatic therapies for the motor symptoms of PD (at least in the early stages of the disease), there are not effective therapies for the non-motor, PD and the commonly co-morbid, Lewy body dementia (LBD). This unmet medical need is identified as one of the FY19 PRP Focus Areas - Mechanisms of non-motor symptoms of PD from basic biology to clinical application. This gap in clinical care reflects our poor grasp of disease mechanisms. While it is widely accepted that mitochondrial dysfunction, synucleinopathy and inflammation contribute to PD and LBD, it is far from clear why these disease mechanisms manifest themselves in some neuronal populations and not others. All neurons rely upon proper protein handling. All neurons depend upon mitochondrial function. All neurons appear to be susceptible to the production of inflammatory cytokines and reactive oxygen species by non-neuronal cells. Understanding the basis for this selective vulnerability could provide the insight needed to develop new, potent therapies for nonmotor symptoms in PD. One of the most vulnerable types of neuron in PD, LBD and Alzheimer's disease (AD) is the basal for brain cholinergic neuron (BFCN). Release of acetylcholine (ACh) by BFCNs modulates the activity of large cortical networks, and the degeneration of these neurons is widely thought to be a primary driver of the cognitive deficits accompanying PD, LBD and AD. Yet, very little is known about how or why these neurons should be vulnerable to mitochondrial dysfunction, synucleinopathy or inflammation.

15. SUBJECT TERMS None listed.					
16. SECURITY CLASSIFICATION OF:			17. LIMITATION OF ABSTRACT	18. NUMBER OF PAGES	19a. NAME OF RESPONSIBLE PERSON USAMRDC
a. REPORT Unclassified	b. ABSTRACT Unclassified	c. THIS PAGE Unclassified	Unclassified	13	19b. TELEPHONE NUMBER *(include area code)*

Standard Form 298 (Rev. 8-98)
Prescribed by ANSI Std. Z39.18

TABLE OF CONTENTS

1. **Introduction:**
Parkinson's disease (PD) and Lewy Bodies dementia (LBD) pose a major healthcare challenge affecting millions of people worldwide. Since age is a primary risk factor for both these conditions, the incidence is projected to steadily rise along with the increase longevity of the population. The absence of disease-modifying therapies and effective symptomatic treatments originate from our poor understanding of the mechanisms driving pathogenesis in PD and LBD. Hallmarks of PD and LBD are synucleinopathy, mitochondrial dysfunction and inflammation. However, how these changes are linked to selective neuronal disfunction is poorly understood. BFCNs are among the most vulnerable neurons in PD and LBD and their degeneration is thought to be responsible for the non-motor cognitive dysfunction in patients. This grant application is designed to begin understand some of the intrinsic and extrinsic determinant of BFNCs vulnerability in the context of synucleinopathies.

2. **Keywords:**
Dementia, Alzheimer's disease, Aging, metabolic syndrome, metabolism regulation, cholinergic, bioenergetics, Agnosia, Anomia, Frontotemporal dementia, vascular dementia, sleep/wake, dysphagia.

3. **Accomplishments:**

What were the major goals of the project?

Our primary research goal is to systematically attack this question using an array of newly developed methodologies that provide an unprecedented capacity to rigorously characterize the genetic, bioenergetic, physiological and anatomical determinants of selective neuronal vulnerability**.** With these powerful tools in-hand, we propose to pursue three specific aims:

Specific Aim 1: *To characterize how autonomous and synaptically-driven activity is generated in BFCNs.* A primary driver of vulnerability is likely to lie in the physiological phenotype of BFCNs – that is, in the traits required for them to fulfill their role in coordinating the activity of large scale cortical and hippocampal networks. The proposed studies employ an advanced array of electrophysiological and optical approaches in conjunction with anatomical methods to characterize two key types of BFCNs in transgenic mice. To provide a molecular anchor to this functional analysis, RiboTag and single-cell RNA harvesting methods will be used in conjunction with RNASeq and quantitative polymerase chain reaction (qPCR) approaches to characterize BFCNs.

Specific Aim 2: *To characterize the relationship between regenerative activity and bioenergetic control in BFCNs*. Our working hypothesis is that the combination of sustained regenerative activity and a massive axonal arbor elevates bioenergetic demand in BFCNs, resulting in sustained mitochondrial oxidant stress that increases synuclein misfolding and susceptibility to inflammation, particularly with advanced age. To test this hypothesis, an array of electrophysiological, optical and genetic strategies will be employed to study the bioenergetic control mechanisms and resulting oxidant stress in somatodendritic and axonal regions of BFCNs from transgenic mice.

Specific Aim 3: To determine the consequences of local and regional synucleinopathy on BFCNs. A hallmark of PD and LBD is the accumulation of misfolded forms of alpha-synuclein (αSYN). Our working hypothesis is that synucleinopathy engages both cell autonomous and non-autonomous (extrinsic) mechanisms to induce BFCN degeneration in PD and LBD. As a first step toward testing this hypothesis, αSYN pre-formed fibrils will be stereotaxically introduced and the functional impact on BFCNs determined using a combination of electrophysiological and optical approaches in transgenic mice. These studies will provide the first clear assessment of αSYN-induced pathophysiology in BFCNs and in so doing should point to strategies for mitigating it.

What was accomplished under these goals?

Specific Aim 1: *To characterize how autonomous and synaptically-driven activity is generated in BFCNs.*

Previously, we reported that pre-incubation with the relatively non-specific NOS inhibitor L-NAME lowered basal spiking rates of BFCNs. However, pre-incubation with the specific neuronal NOS inhibitor (nNOS) generated by the Silverman group (HD-3-86) failed to confirm this result, arguing that inhibition of nNOS has no effect on basal spiking rates in BFCNs. This result is consistent with those described below which show that nNOS is activated in BFCNs when they are induced to spike at rates roughly twice those at baseline. At these higher spike rates, Ca^{2+} entry stimulates nNOS and NO signaling to enhance ryanodine receptor mediated Ca^{2+} entry into mitochondria and oxidative phosphorylation (OXPHOS). As described below, this activity-dependent engagement of nNOS signaling serves as metabolic switch in BFCNs away from glycolysis to OXPHOS.

As described in the previous progress report, high frequency optogenetic stimulation of D1 SPN afferent input to BFCN evokes a biphasic response consisting of an initial $GABA_A$ receptor mediated inhibition of spiking followed by a sustained increase in spiking for seconds (Fig. 1A). Our initial hypothesis was that the persistent elevation in spiking was attributable to release of substance P (SP) from D1 SPN terminals and activation of postsynaptic tachykinin/neurokinin 1 receptors (NK1Rs). Our transcriptomic profiling of BFCNs confirmed the expression of *TACR1* mRNA. Consistent with this hypothesis, pre-incubation of ex vivo brain slices with the NK1R antagonist L703 606 attenuated the elevation in BFCN spiking following optogenetic stimulation of D1 SPN axons (Fig. 1A-C). However, the NK1R antagonist only partially blocked the D1 SPN evoked elevation in spiking. At glutamatergic synapses it has been reported that vesicular proton release following burst stimulation can activate postsynaptic, voltage-insensitive, acid-sensitive ion (ASIC) channels (Wemmie et al., 2013). Indeed, our transcriptomic profiling of BFCNs revealed robust expression of genes coding for two of the five types of ASIC channels (*ASIC2, ASIC4*). To test for their involvement in the response to D1 SPNs, the ASIC channel blocker amiloride was bath applied prior to measuring the change in BFCN spiking evoked by optogenetic stimulation of D1 SPN axons. Amiloride attenuated the elevation in spiking rate produced by sustained stimulation of D1 SPN axons (Fig. 2A). However, as with the

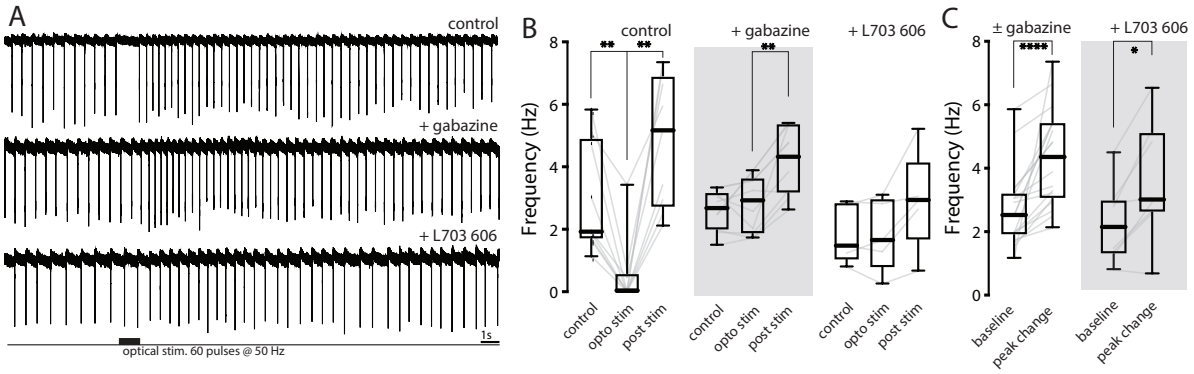

Figure 1: **Optogenetic stimulation of D1-SPN axons evokes a multiphasic response in BFCNs**. A. Representative traces showing cell-attached recording of BFCN activity following high-frequency optical stimulation (1 ms pulse duration delivered 60 times at 50 Hz) with a 470 nm LED of D1-SPN axons; this stimulation resulted in a short pause followed by a delayed acceleration of BFCN firing activity in control (in the presence of the ionotropic glutamate receptor antagonist cyanquixaline (6-cyano-7-nitroquinoxaline-2,3-dione (CNQX); 10 μM, upper). Bath applied gabazine (20 μM for 2 min, middle) abolished the short pause, and bath applied L703 606 (1 μM for 5-10 min, lower) partially blocked the delayed acceleration in BFCN activities. B. Box plots summarizing BFCN spiking frequency before, during, and after the optical stimulation in control CNQX (left, ** p <0.01, n = 9) followed by bath applied gabazine (mid, ** p < 0,01 n = 22), and L703 606 (right, n = 5). C. Box plots comparing maximum increase of BFCN spiking frequency following D1-SPN stimulation in control (left, **** p < 0.0001, n = 18) and L703 606 (right, * p <0.05, n = 8) both with and without gabazine. Box plots represent the median (thick like) and interquantile range, whiskers represent maximum and minimum.

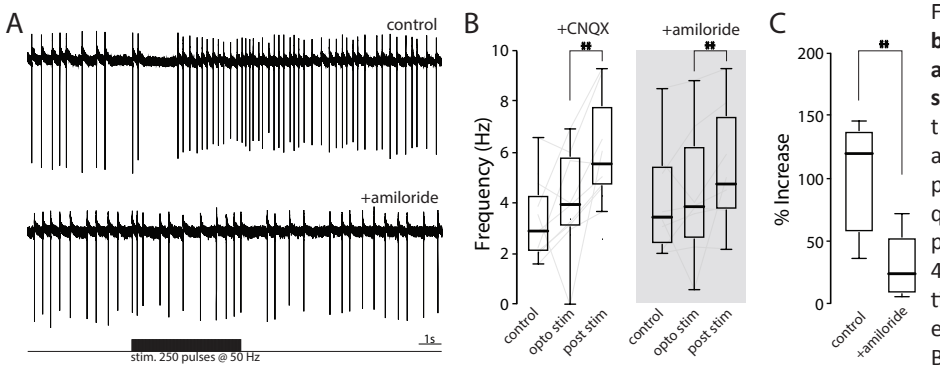

Figure 2: **A nonselective ASICs inhibitor partially blocks the delayed enhancement of BFCN excitability induced by the repetitive high-frequency stimulation of D1-SPN axons**. A. Representative traces showing cell-attached recordings of BFCN activity in control CNQX (10 μM, upper) or bath applied amiloride (200 μM, lower) following high-frequency optical stimulation on D1-SPN axons (1 ms pulse duration delivered 250 times at 50 Hz) with a 470 nm LED. Due to an extended period of stimulation, GABAA receptor activation was lost before the end of the stimulation, and BFCN resumed spiking. B. Box plots summarizing BFCN spiking frequency before, 1 second after stimulation started, and after the optical stimulation recorded in the presence of CNQX (left, ** p<0.01, n = 9) or amiloride (right, ** p<0.01, n = 8) C. Box plots comparing the percent increase in BFCN spiking following D1-SPN stimulation recorded in control (+CNQX) (left) and amiloride (right, ** p<0.01, n = 8).

NK1R antagonist, the attenuation in the post-stimulation elevation is spiking by amiloride (summarized for experiments in the presence of gabazine) was only partial (Fig. 2B, C). Taken together, these results suggest that the D1 SPNs release both SP and protons to activate postsynaptic NK1Rs and ASIC2/4s, resulting in a sustained elevation in BFCN spiking. Thus, when robustly activated, D1 SPNs can produce a sustained increase in BFCN spiking, leading to arousal and cortical synchronization.

Specific Aim 2: *To characterize the relationship between regenerative activity and bioenergetic control in BFCNs.*

Over the past year, our studies have built out the mechanisms responsible for bioenergetic control in BFCNs, and how NO signaling modulates these mechanisms. Using a adenoassociated virus (AAV) delivery of a Cre-dependent expression cassette for the optical sensor of ATP/ADP ratio (PercevalHR) in ChAT-Cre mice and two photon laser scanning microscopy (2PLSM) in ex vivo brain slices (Fig. 3A,B), we confirmed that, in the absence of exogenous stimulation, cytosolic ATP maintenance in BFCNs is heavily reliant upon glycolysis, in contrast to other at-risk neurons, like substantial nigra pars compacta (SNc) dopaminergic neurons (Fig. 3C,D). As shown in Fig. 3C, inhibition of complex V (and mitochondrial ATP production) has a very modest effect on cytosolic ATP/ADP ratio, in contrast to the situation in SNc dopaminergic neurons and striatal cholinergic interneurons. This balance between glycolysis and OXPHOS is captured in the OXPHOS index (Zampese et al., 2022). This ratio is significantly lower in BFCNs, than in either SNc dopaminergic neurons or cholinergic interneurons (Fig.

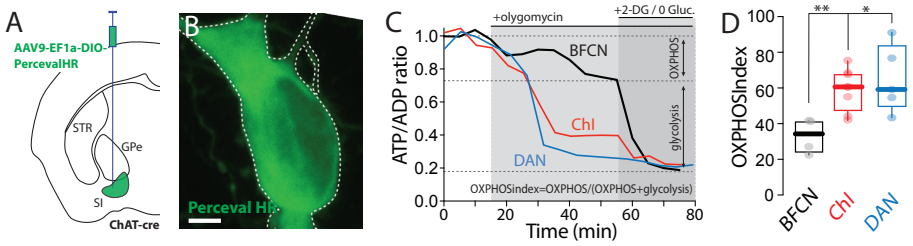

Figure 3. **Bioenergetic role of mitochondrial oxidative phosphorylation in BFCNs during baseline activity.** A. Schematic representing the viral delivery strategy to selectively express PercevalHR in BFCNs by injecting a cre-dependent PercevalHR viral construct in the BF of ChAT-Cre mice. B. Representative 2-PLSM image of a BFCN expressing PercevalHR (scale bar, 10 µm). C. Representative PercevalHR time-lapse experiments measuring ATP/ADP ratio in BFCNs (black trace), striatal cholinergic interneuron (ChI; red trace), and SNc dopaminergic neurons (DAN, blue trace); bath application of mitochondrial complex V inhibitor oligomycin (10 µM) was used to estimate the contribution of mitochondria to the ATP/ADP ratio, while substitution of glucose with the non-hydrolysable analogue 2-deoxyglucose (2-DG, 3.5 mM) was used to estimate the glycolytic contribution to the ATP/ADP ratio. The relative contribution of mitochondria to the ATP/ADP ratio was quantified as "OXPHOS index", i.e. the oligomycin-sensitive drop in the ATP/ADP ratio versus the total drop observed upon inhibition of both glycolytic and mitochondrial ATP production. D. Box plots summarizing the OXPHOS index at baseline for BFCNs, ChIs and SNc dopaminergic neurons (DANs) (n=4, 7, 5 respectively; *p<0.05, **p<0.01). Box plots represent the median (thick like) and interquartile range, whiskers represent maximum and minimum.

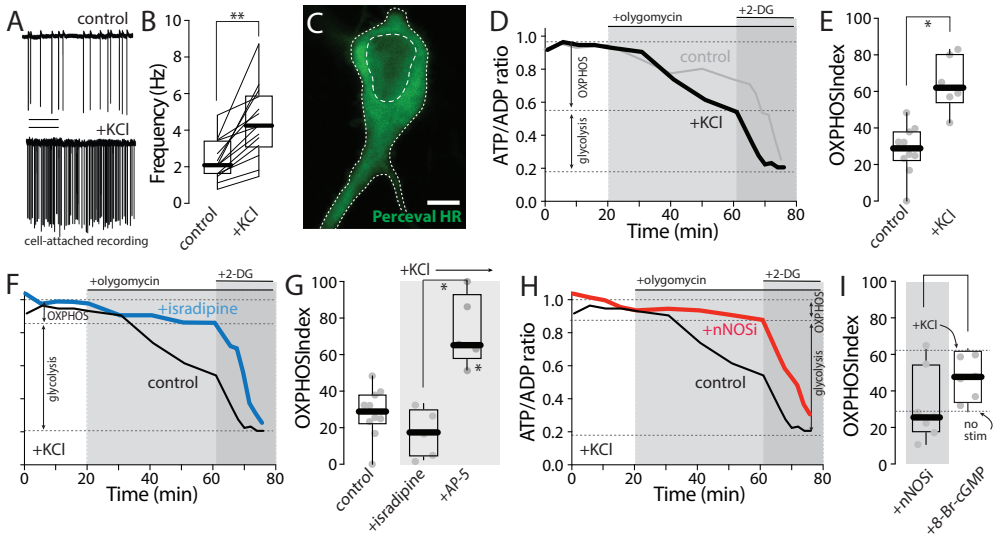

Figure 4. **Ca2+- and NO- mediated increase in mitochondrial ATP production in BFCNs upon increases in spike rate.** A. Representative cell-attached recordings from BFCNs in control conditions or in higher KCl (+KCl, 6 mM) B. Box plots summarizing the increase in spike rate in higher KCl compared to control conditions (n = 14, ** p <0.01) C. Representative 2-PLSM image of a BFCN expressing PercevalHR (scale bar, 10 µm). D. Representative PercevalHR time-lapse experiments measuring the ATP/ADP ratio in BFCNs in control conditions (gray trace) or upon increased spike rate (KCl 6 mM, black trace). Bath application of oligomycin (10 µM) and substitution of glucose with 2-DG (3.5mM) were used to estimate the contribution of mitochondria to the ATP/ADP ratio, as in Figure 3. E. Box plots showing an increase in OXPHOS index when BFCNs are induced to fire at higher spike rate (+KCl) versus control conditions (n=10, 6 respectively; p<0.05). F. Representative PercevalHR time-lapse experiments measuring changes in the ATP/ADP ratio in BFCNs stimulated to fire at increased spike rate (+KCl) in control conditions or upon pre-incubation with the Cav1 negative allosteric modulator isradipine (1 µM). G. Box plots illustrate that treatment with isradipine but not with the NMDA receptor antagonist AP-5 (50 µM) prevents the increase in OXPHOS index observed in BFCNs upon KCl stimulation (n=10, 4, 5 respectively; p<0.05). H. Representative PercevalHR time-lapse experiments measuring changes in the ATP/ADP ratio in BFCNs stimulated to fire at increased spike rate (+KCl) in control conditions or treated with the nNOS specific inhibitor HD-3-86 (nNOSi, 100 nM). I. Box plots illustrate that in BFCNs treatment with nNOSi prevents the increase in the OXPHOS index observed during KCl stimulation (dashed line), and conversely that activating PKG with bath application of 8-bromo-cGMP (8-Br-cGMP, 10 µM) increases BFCNs OXPHOS index in absence of stimulation (n= 8, 7 respectively). Box plots represent the median (thick like) and interquantile range, whiskers represent maximum and minimum.

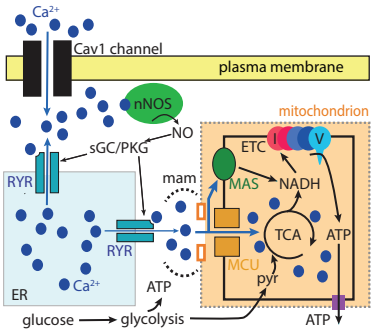

Figure 5: **Schema of the intracellular signaling pathways linking Cav1 channels to OXPHOS.** Abbreviations: MCU=mitochondrial uniporter; TCA=tricarboxylic acid cycle; MAS=malate-aspartate shuttle; NADH=nicotinamide adenine dinucleotide (NAD) + hydrogen (H); ATP=adenosine triphosphate; ETC=electron transport chain; PKG=protein kinase G; sCG=soluble guanylyl cyclase. Other abbreviations as in text.

3D).

To determine if the reliance upon glycolysis in BFCNs persisted when ATP demand increased, their basal spiking rate was increased by elevating the extracellular K^+ concentration. This shift roughly doubled spiking rate (Fig. 4A,B), much like the change in rate achieved by optogenetic stimulation of D1 SPN afferents to BFCNs (see above). As above, PercevalHR was expressed in BFCNs using an AAV vector and a Cre-dependent expression construct (Fig. 4C). At the higher, KCl driven spiking rate, BFCNs significantly increased their engagement of mitochondrial OXPHOS to maintain cytosolic ATP/ADP ratio (Fig. 4D); indeed, their OXPHOS index rose into the range found in SNc dopaminergic neurons (Fig. 4E).

In SNc dopaminergic neurons, the activity-dependent elevation in mitochondrial OXPHOS is driven by Ca^{2+} entry through depolarization-activated, plasma membrane Cav1 channels (Zampese et al., 2022). Similarly, in BFCNs, the KCl-driven elevation in OXPHOS was blunted by inhibiting Cav1 Ca^{2+} channels with the negative allosteric modulator isradipine, whereas the NMDA receptor antagonist AP-5 had no effect on OXPHOS (Fig. 4F, G). With the KCl-driven elevation in OXPHOS, mitochondrial oxidant stress rose and was lowered to control levels by isradipine (data not shown).

In other cell types, Ca^{2+} entry through Cav1 channels can stimulate nNOS, leading to NO-dependent regulation of a variety of cellular functions linked to bioenergetics. To probe the potential role of NO signaling in BFCNs, the NO donor S-nitroso-N-acetyl-penicillamine (SNAP) was bath applied while monitoring intracellular Ca^{2+} oscillations triggered by spiking; this was accomplished in *ex vivo* brain slices from ChAT-GFP mice by dialyzing Fluo4 into visually identified through a patch pipette and then monitoring fluorescence using 2PLSM. Interestingly, SNAP increased the spike-associated Ca^{2+} transient and this effect was blocked by the ryanodine receptor (RYR) antagonist DHBP and mimicked by the membrane permeable cyclic guanosine monophosphate (cGMP)c analog 8-bromo-cGMP (data not shown). These results suggest that Ca^{2+}-induced Ca^{2+} release of endoplasmic reticulum Ca^{2+} stores through RYRs, which is known to regulate mitochondrial OXPHOS (Zampese et al. 2022) was being controlled by nNOS and the NO signaling cascade through guanylyl cyclase (GC) and protein kinase G (PKG). Previous work has shown that PKG can phosphorylate RYRs to enhance Ca^{2+} dependent opening (Gonano et al., 2023) To test this hypothesis, the ability of the nNOS specific inhibitor (HD-3-86) to blunt the KCl-driven elevation in OXPHOS was tested using PercevalHR (as above). Indeed, nNOS inhibition prevented the activity-dependent engagement of mitochondrial OXPHOS (Fig. 4H). Moreover, the mitochondrial contribution to ATP production was enhanced in unstimulated BFCNs by bath application of 8-bromo-cGMP (Fig. 4I). Taken together, these data suggest that nNOS and NO signaling acts as an activity-dependent bioenergetic switch in BFCNs, inducing an elevation in OXPHOS with increased spiking by controlling the gain of feedforward regulation (Fig. 5).

Specific Aim 3: *To determine the consequences of local and regional synucleinopathy on BFCNs.*

Weeks after stereotaxic injection of pre-formed fibrils of aSYN (PFFs) into the BF, BFCN firing rate is significantly elevated (measured with patch clamp techniques in ex vivo brain slices) and this change is reversed by the anti-oxidant N-acetyl-cysteine (NAC) (Fig. 6A-C). As predicted by the work described above, the increase in discharge rate is accompanied by a switch to OXPHOS in BFCNs as measured with the approaches described above (Fig. 6D, E). This metabolic switch is accompanied by an expected elevation in mitochondrial oxidant stress measured using the genetically encoded optical sensor mito-roGFP and 2PLSM in ex vivo brain slices (Fig. 6F, G); mito-roGFP was expressed specifically in BFCNs by AAV delivery of a Cre-dependent mito-roGFP expression construct in an AAV vector. As predicted, the mitochondrial oxidant stress seen in the presence of PFFs was reversed by inhibiting Cav1 channels with isradipine or diminishing ROS signaling with NAC (Fig. 6G). Given the sensitivity of the change in spike rate on NAC, it is possible that release of superoxide by neighboring activated microglia was responsible (microglial activation by PFFs was shown previously). However, measurements of cytosolic oxidant stress in BFCNs using cyto-roGFP (Graves et al., 2020) (using similar methods to those described above) failed to detect any shift following PFF deposition (Fig. 6H-J).

These results suggest that PFF-activated microglia (or astrocytes) are releasing inflammatory cytokines that drive increased spiking in BFCNs. One prominent cytokine released by microglia is TNFalpha (TNFa). Moreover, microglial and astrocytic release of TNFa has been reported to be blocked by NAC (Pahan et al., 1998; Sakai et al., 2023). In our transcriptomic work, several members of the TNFa receptor superfamily were found to be expressed in BFCNs, including *TNFRSF1a, TNFRSF19, and TNFRSF21*. Indeed, bath application of TNFa reversibly accelerated basal spiking rate of BFCNs (Fig. 6K, L). This elevation in spiking rate was accompanied by the expected shift to mitochondrial OXPHOS (Fig. 6M, N)

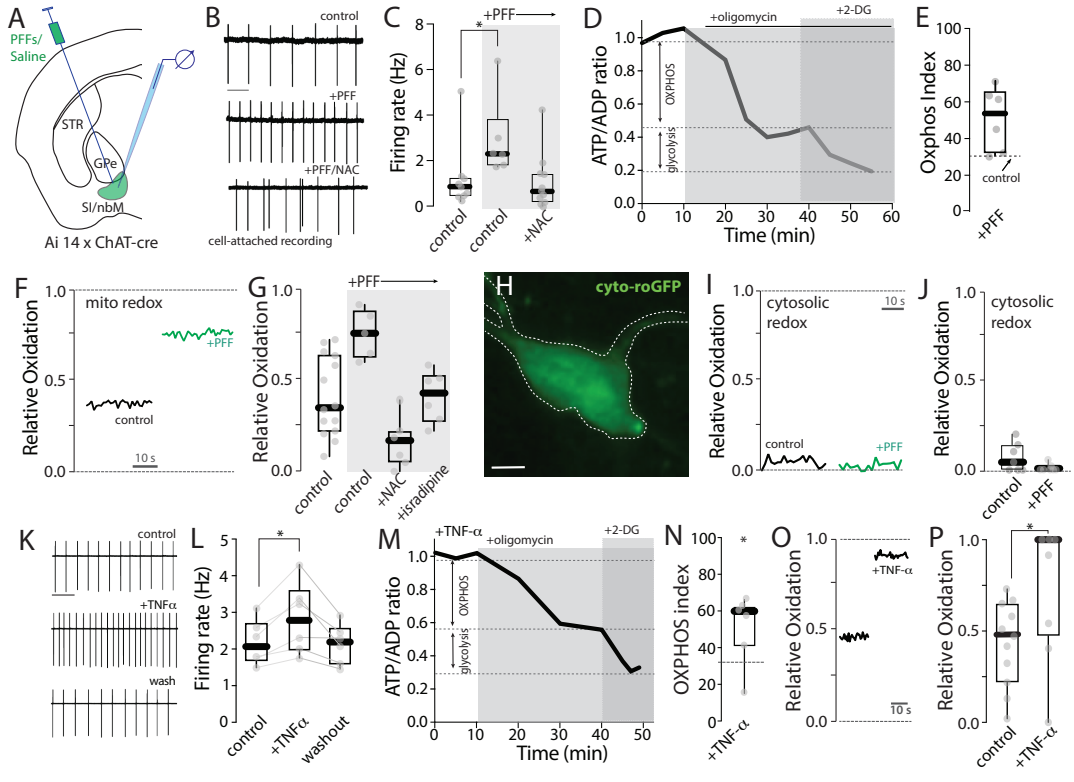

Figure 6. **PFF-induced inflammation increases BFCNs firing rate and mitochondrial stress.** A. Schematic representing the strategy to deliver PFF to the basal forebrain; saline injection is used as control. B. Representative cell-attached recordings from BFCNs in control conditions and in PFF-injected mice with or without NAC (500 µM) treatment. C. Box plots summarizing the spike rate in BFCNs in control condition, in slices from PFF-injected mice, with or without NAC treatment (n=9, 11, 6 respectively, $p < 0.01$). D. Representative PercevalHR time-lapse experiment measuring the ATP/ADP ratio in BFCNs in slices from mice that received PFF injections in the basal forebrain. Bath application of oligomycin (10 µM) and substitution of glucose with 2-DG (3.5 mM) were used to estimate the contribution of mitochondria to the ATP/ADP ratio, as in Figure 3. E. Box plot showing the higher OXPHOS index measured in BFCS from PFF-injected mice (n = 6) compared to control conditions (dashed line). F. Representative mito-roGFP measurements after calibration in BFCNs from control and PFF-injected mice. G. Box plots showing higher mitochondrial relative oxidation in BFCNs from PFF-injected mice versus controls; treatment with the anti-oxidant NAC (500 µM) or the Cav1 negative allosteric modulator isradipine (1 µM) decreases the PFF-induced elevation in mitochondrial oxidant stress (n= 14, 5, 5, 6 respectively). H. Representative 2-PLSM image of a BFCN expressing cyto-roGFP (scale bare, 10 µm). I. Representative cyto-roGFP measurements after calibration in BFCNs from control and PFF-injected mice J. Box plots showing comparable cytosolic relative oxidation in BFCNs from PFF-injected mice versus controls (n =7, 7 respectively). K. Representative cell-attached recordings from BFCNs in control conditions, during TNF-a (10 nM) bath application, and after its washout. L. Box plots summarizing the spike rate in BFCNs in control conditions, during TNF-a (10 nM) bath application, and after its washout (n=6, $p < 0.05$) M. Representative PercevalHR time-lapse experiment measuring the ATP/ADP ratio in BFCNs treated with the inflammatory cytokine TNF-a (10 nM). N. Box plot showing the higher OXPHOS index measured in BFCS treated with TNF-a (n = 6, $p<0.05$ Mann-Whitney test) compared to control conditions (dashed line)¬¬. O. Representative mito-roGFP measurements after calibration in BFCNs treated with TNF-a and controls. P. Box plots showing higher mitochondrial relative oxidation in BFCNs treated with TNF-a and versus controls (n=7, 11, respectively; $p<0.05$ Mann-Whitney test). Box plots represent the median (thick like) and interquantile range, whiskers represent maximum and minimum.

and a dramatic increase in mitochondrial oxidant stress (Fig. 6O, P). Even though BFCNs did not manifest PFF-induced pathology in our experiments, had the exposure to PFF-induced inflammation been maintained for a longer period it may have appeared. Our studies show that inflammation and TNFα release excites BFCNs, driving metabolism toward OXPHOS. The resulting elevation in mitochondrial oxidant stress could compromise proteostasis, leading to accumulation of misfolded proteins (e.g., oligomeric aSYN, tau). Oxidant stress can also result in damage to mitochondrial DNA (mtDNA), which, if released, can promote inflammation and PD-like pathology (Tresse et al. 2023) This hypothetical cascade of events is summarized in Figure 7. Lastly, it is interesting to note that recent work suggests that elevated TNFa signaling is central to pathogenesis in PD dementia (Villanueva et al., 2021).

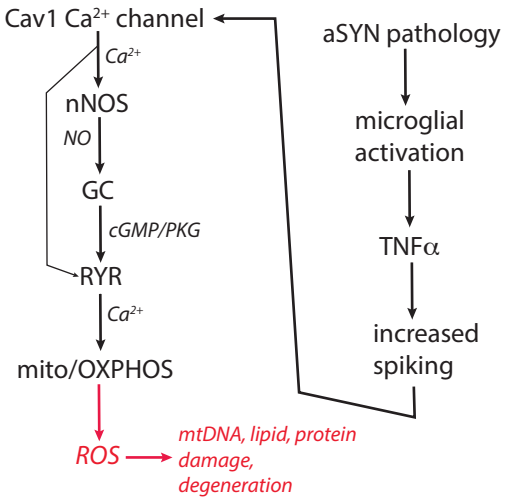

Figure 7: **Hypothetical signaling cascade linking PFF-induced inflammation to a sustained elevation in NO production and mitochondrial oxidant stress.** A sustained elevation in oxidant stress has been linked to mitochondrial deoxyribonucleic acid (mtDNA) damage, lipid and protein damge and neurodegeneration.

References:

Gonano, L. A. *et al.* Regulation of cardiac ryanodine receptor function by the cyclic-GMP dependent protein kinase G. *Curr. Res. Physiol.* **5**, 171–178 (2022).

Graves, S. M. *et al.* Dopamine metabolism by a monoamine oxidase mitochondrial shuttle activates the electron transport chain. *Nat Neurosci*

23, 15–20 (2019).
Pahan, K., Sheikh, F. G., Namboodiri, A. M. S. & Singh, I. N-Acetyl Cysteine Inhibits Induction of No Production By Endotoxin or Cytokine Stimulated Rat Peritoneal Macrophages, C6 Glial Cells and Astrocytes. *Free Radic. Biol. Med.* **24**, 39–48 (1998).
Sakai, M. *et al.* N-Acetylcysteine Suppresses Microglial Inflammation and Induces Mortality Dose-Dependently via Tumor Necrosis Factor-α Signaling. *Int. J. Mol. Sci.* **24**, 3798 (2023).
Tresse, E. *et al.* Mitochondrial DNA damage triggers spread of Parkinson's disease-like pathology. *Mol. Psychiatry* 1–13 (2023) doi:10.1038/s41380-023-02251-4.
Villanueva, E. B. *et al.* Neuronal TNFα, Not α-Syn, Underlies PDD-Like Disease Progression in IFNβ-KO Mice. *Ann. Neurol.* **90**, 789–807 (2021).
Wemmie, J. A., Taugher, R. J. & Kreple, C. J. Acid-sensing ion channels in pain and disease. *Nature reviews Neuroscience* **14**, 461 471 (2013).
Zampese, E. *et al.* Ca2+ channels couple spiking to mitochondrial metabolism in substantia nigra dopaminergic neurons. *Sci Adv* **8**, (2022).

What opportunities for training and professional development has the project provided?
Nothing to Report

How were the results disseminated to communities of interest?
Nothing to Report

What do you plan to do during the next reporting period to accomplish the goals?
Our plan is to continue with the research plan outlined in the original proposal.

4. Impact:

What was the impact on the development of the principal discipline(s) of the project?
Nothing to Report

What was the impact on other disciplines?
Nothing to Report

What was the impact on technology transfer?
Nothing to Report

What was the impact on society beyond science and technology?
Nothing to Report

5. Changes/Problems:

Changes in approach and reasons for change
Nothing to Report

Actual or anticipated problems or delays and actions or plans to resolve them
Nothing to Report

Changes that had a significant impact on expenditures
None

Significant changes in use or care of human subjects, vertebrate animals, biohazards, and/or select agents
None

Significant changes in use or care of human subjects
Not applicable.

Significant changes in use or care of vertebrate animals.
None

Significant changes in use of biohazards and/or select agents
Not applicable.

6. Products:

Publications, conference papers, and presentations
Nothing to Report

Journal publications.
Nothing to Report

Books or other non-periodical, one-time publications.
Nothing to Report

Other publications, conference papers, and presentations.
Nothing to Report

Website(s) or other Internet site(s)
Nothing to Report

Technologies or techniques
Nothing to Report

Inventions, patent applications, and/or licenses
Nothing to Report

Other Products
Nothing to Report

7. Participants & Other Collaborating Organizations

What individuals have worked on the project?

Name:	D. James Surmeier, PhD
Project Role:	PI
Researcher Identifier (e.g. ORCID ID):	
Nearest person month worked:	2
Contribution to Project:	Oversees the carrying out of the research plan to ensure all aims and goals are met. Works closely with the investigative team to develop experimental plans that test the proposed hypothesis, analyzes data from experiments, and leads the overall manuscript development process.

Name:	Tristano Pancani, PhD
Project Role:	Co-Investigator
Researcher Identifier (e.g. ORCID ID):	0000-0003-0511-7702
Nearest person month worked:	6
Contribution to Project:	Responsible for the conduct of the work proposed in Specific Aim 2, part of Specific Aim 3 and Specific Aim 4.

Name:	Tatiana Tkatch, PhD
Project Role:	Co-Investigator
Researcher Identifier (e.g. ORCID ID):	
Nearest person month worked:	5
Contribution to Project:	Responsible for the conduct of Specific Aim 1 and portions of Specific Aim 4.

Name:	Jaime Guzman-Lucero, PHD
Project Role:	Co-Investigator
Researcher Identifier (e.g. ORCID ID):	0000-0002-1746-8537
Nearest person month worked:	4
Contribution to Project:	Responsible for assisting with the experiments in Specific Aim 2 and for conducting the experiments outlined in Specific Aim 3. He assists with experimental design, data analysis, manuscript development, and works closely with the rest of the investigative team.

Has there been a change in the active other support of the PD/PI(s) or senior/key personnel since the last reporting period?

New Active awards:

- Cure Parkinson's Trust, PI: Surmeier, began 3/1/23, effort 0.06 CM

Completed awards:

- William N. & Bernice E. Bumpus Foundation, Agreement Letter 07/05/2018, PI: Surmeier, ended 6/2022
- NIH/NIMH, R01MH099114, PI: Contractor, ended 1/2023
- MJFF, MJFF-019948, PI: Surmeier, ended 7/2023
- MJFF, MJFF-019886, PI: Chandel, ended 8/2023

What other organizations were involved as partners?

Nothing to Report.

8. Special Reporting Requirements

Attached.

9. Appendices:

Not applicable.